Journal of the Ceramic Society of Japan 124 [8] 838-840 2016 Note

High-strength pseudobrookite-type $MgTi_2O_5$ by spark plasma sintering

Hyoung-Won SON,[*] Ryosuke S. S. MAKI,[*] Byung-Nam KIM[**] and Yoshikazu SUZUKI[*,*,†]**

[*]Graduate School of Pure and Applied Sciences, University of Tsukuba, 1–1–1 Tennodai, Ibaraki 305–8573, Japan
[**]Material Processing Unit, National Institute for Materials Science, 1–2–1 Sengen, Tsukuba, Ibaraki 305–0047, Japan
[***]Faculty of Pure and Applied Sciences, University of Tsukuba, 1–1–1 Tennodai, Ibaraki 305–8573, Japan

Bulk polycrystalline $MgTi_2O_5$ has low coefficients of thermal expansion (CTE), high thermal shock resistance and high temperature stability. However, polycrystalline $MgTi_2O_5$ generally includes extensive internal microcracks and hence it has poor mechanical properties. In this study, dense $MgTi_2O_5$ samples with fewer microcracks were prepared by spark plasma sintering (SPS) of commercially available $MgCO_3$ (basic) and TiO_2 (anatase) powders at 1000–1200°C for 20 min under 20–80 MPa in vacuum. The samples sintered above 1100°C were composed of $MgTi_2O_5$ phase with trace intermediate $MgTiO_3$. High relative density and flexural strength, 99.9% and 341.5 MPa, were obtained for the samples sintered at 1200°C under 80 MPa. This strength value is, to the best of our knowledge, the highest value among pseudobrookite-type ceramics. The bulk CTE values of the samples were almost identical for all samples, ~10 × 10^{-6} K^{-1}, which confirms the fewness of microcracks.

Key-words : Pseudobrookite, $MgTi_2O_5$, SPS, Thermal expansion, Flexural strength

[Received March 9, 2016; Accepted May 21, 2016]

$MgTi_2O_5$ ceramics, having the orthorhombic pseudobrookite structure [**Fig. 1**, space group *C*mcm (63)], exhibit large thermal expansion anisotropy.[1)–4)] The coefficients of thermal expansion (CTE) of pseudobrookite structure are typically negative or very small in the *a*-direction, moderate in *b*-direction (~10 × 10^{-6} K^{-1}) and rather large in *c*-direction (~15–20 × 10^{-6} K^{-1}). The low thermal expansion was found for bulk $MgTi_2O_5$ ceramics due to the presence of extensive internal microcracks formed by thermal stress during the sintering.[1)] They generally have poor mechanical properties due to the microcracks, and hence, the commercial applications have been limited.

Kusuzyk and Bradt[5)] reported the effects of grain size on thermal expansion anisotropy in $MgTi_2O_5$; $MgTi_2O_5$ powder was hot-pressed in a graphite die at 20.7 MPa and 1200°C for 1 h. Reported maximum flexural strength and density of the sintered parts were 116 MPa and 3.60 g/cm^3 (98.4% of theoretical), respectively. To the best of our knowledge, it was the highest flexural strength of $MgTi_2O_5$ ceramics. However, this flexural strength is not sufficient for general structural applications.

Among the pseudobrookite-type ceramics, aluminum titanate (Al_2TiO_5) has been widely studied,[6),7)] in particular on the improvement of the mechanical properties. Ohya et al.[7)] reported the effect of some additives on microstructure and flexural strength of Al_2TiO_5 ceramics. Al_2TiO_5–5 wt% MgO powder was sintered at 1300–1400°C after CIP under 98 MPa. The maximum flexural strength was 181.4 MPa of the sample sintered at 1350°C. It was probably the highest flexural strength among pseudobrookite-type ceramics. However, this mechanical property is also not sufficient for typical structural applications. Moreover, Al_2TiO_5 is thermodynamically metastable under 1200°C and it gradually decomposes into Al_2O_3 and TiO_2.[8)–10)]

Spark plasma sintering (SPS) [or pulsed electric current sintering (PECS)] is effective for full densification.[11)] Compared with conventional sintering, SPS enables (1) rapid heating (~200°C/min), (2) densification at lower temperatures (and hence, less grain growth), (3) short sintering time and (4) enhanced mass transport (via electromigration).[12)–14)] Here, in this study, we report highly dense and strong pseudobrookite-type $MgTi_2O_5$. The samples were reactively sintered by SPS for the efficient densification, and were characterized by Archimedes' method, XRD, 3-point bending test, SEM, and thermo-mechanical analysis of the CTE.

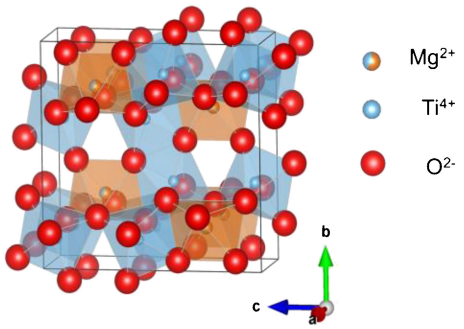

Fig. 1. The crystal structure of $MgTi_2O_5$.

Commercially available $MgCO_3$ (basic) (99.9% up, Kojundo Chemical Laboratory Co. Ltd., Saitama, Japan) and TiO_2 anatase (99%, Kojundo Chemical Laboratory) powders were used as the starting materials.[15)–18)] Powder mixture of $MgCO_3$ (basic) and TiO_2 anatase with molar ratio of 1:2 was prepared by wet ball-milling with Y-doped ZrO_2 media (YTZ, Nikkato Co.) for 24 h using ethanol, and then the slurry was dried in an evaporator. Finally, the mixed powder was dried at 80°C, and then, sieved through a 150 μm screen. The mixed powder was poured into a graphite die and pressed using a 20 mm diameter graphite punch. The samples were reactively sintered using a SPS machine (LABOX-315CS, SinterLand Inc., Japan) at 1000–1200°C for 20

† Corresponding author: Y. Suzuki; E-mail: suzuki@ims.tsukuba.ac.jp

DOI http://dx.doi.org/10.2109/jcersj2.16058

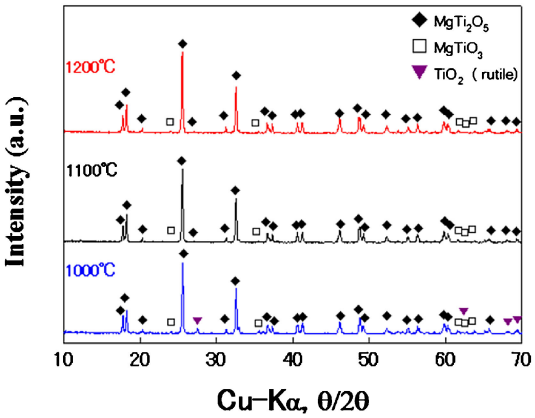

Fig. 2. XRD patterns of $MgTi_2O_5$ samples sintered by SPS at each temperature.

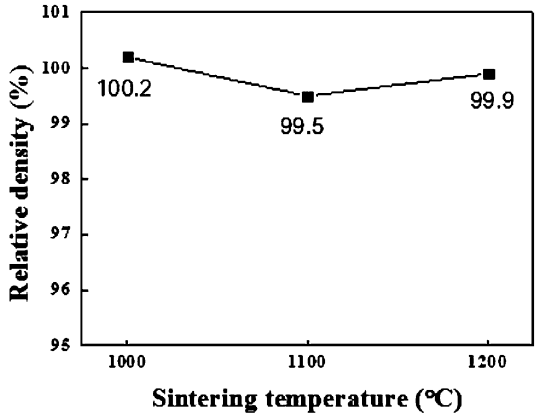

Fig. 3. The relative density of samples sintered at each temperature.

min under a uniaxial pressure of 20–80 MPa in vacuum (10^{-3} torr). After holding at the sintering temperature, the sintered bodies were slowly cooled at a rate of 15°C/min to suppress microcracks in the bulk sample caused by thermal shock during cooling. Finally, the sintered discs, 20 mm in diameter and 3 mm in thickness, were obtained.

The relative densities were analyzed by Archimedes' method. The relative density was nominally calculated using the theoretical density of $MgTi_2O_5$ (3.65 g/cm^3). The constituent phases of sintered samples were analyzed by X-ray powder diffraction (XRD, Rigaku, Multiflex, Cu-K_α, 40 kV and 40 mA). Prior to the powder XRD measurement, the sintered samples were pulverized, and the XRD patterns were collected in the range of $2\theta =$ 10–70°. In order to evaluate flexural strength, sintered samples were machined into the test specimens with dimension of ~3 × 2.5 × 20 mm. The all sides of the each specimen were polished using abrasive paper and diamond slurry, and then, the tensile face and corners of each specimen were polished and chamfered by 0.5 µm diamond slurry and waterproof abrasive paper (P1200, Riken Corundum Co. Ltd. Japan), respectively. Flexural strength was measured by three-point bending test with a span of 16 mm and cross head speed of 0.5mm/min by using a universal testing machine (Autograph AG-20kNIT, Shimadzu Co. Ltd., Japan). Three samples were used for each measurement. Microstructure was observed by scanning electron microscopy (SEM, JSM-5600/SV, JEOL, Japan). The coefficient of thermal expansion (CTE) was evaluated from 50–1000°C by thermomechanical analysis (TMA, Thermo plus EVO II, RIGAKU, Japan).

Figure 2 shows XRD patterns of the $MgTi_2O_5$ samples sintered by SPS at 1000, 1100 and 1200°C for 20 min, respectively. The sample sintered at 1000°C mainly consisted of $MgTi_2O_5$ with some TiO_2 rutile and trace of $MgTiO_3$ phases. On the other hand, the samples sintered at 1100 and 1200°C contained $MgTi_2O_5$ and trace of $MgTiO_3$ phases.

As for normal sintering (without SPS) conditions, Nakagoshi and Suzuki[18] reported the morphology control of pseudobrookite-type $MgTi_2O_5$ powders by LiF doping. The mixture of $MgCO_3$ (basic) and TiO_2 anatase powders were calcined in air at 1100°C for 2 h, and the obtained powder consisted of single-phase $MgTi_2O_5$. At lower SPS sintering temperature (1000°C), some residual (unreacted) $MgTiO_3$ and rutile phases are simply attributable to the insufficient reaction. At higher SPS sintering temperature (1100–1200°C), some residual $MgTiO_3$ phase may be attributed to a reductive atmosphere by carbon in SPS. **Figure 3** shows the relative density of the $MgTi_2O_5$ samples sintered at

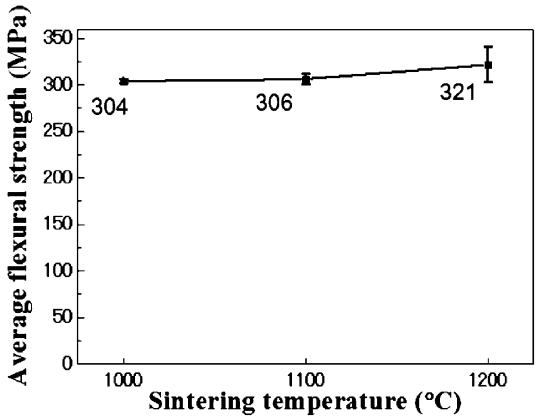

Fig. 4. Flexural strength (3-point bending) of the samples sintered at each temperature.

each temperature. The relative density of all samples was above 99.5%. The extremely high density, 99.9% was obtained when the sample was sintered at 1200°C. Due to the coexistence of TiO_2 rutile phase, the relative density of the sample sintered at 1000°C numerically exceeded 100% (the theoretical densities of $MgTi_2O_5$ and rutile are 3.65 and 4.26 g/cm^3,[9] respectively).

Figure 4 shows the effect of the SPS sintering temperature on the flexural strength of $MgTi_2O_5$ samples. The flexural strength increased with increasing sintering temperature, and the maximum strength, 345.1 MPa, was obtained for the sample sintered at 1200°C. This result was much higher than previous works.[5),7)] The enhancement of the flexural strength can be attributed to its high relative density (~99.9%). However, at the same sintering temperature (1200°C), the standard deviation was somewhat large, which is attributable to some generated microcracks by the anisotropic thermal expansion in the bulk ceramics during the sintering process (including cooling). Thus, from the view point of strength, the optimal reactive sintering temperature for $MgTi_2O_5$ ceramics by SPS should be ~1100°C.

Figure 5 shows SEM images of fracture surface of each sample. The average grain sizes of the samples sintered at 1000, 1100, and 1200°C were ~0.7, ~1.0 and ~1.4 µm, respectively. The origins of the fracture were clearly observed from the SEM images of samples sintered at 1000 and 1200°C. The defect on the fracture surface acted as the stress riser. On the other hand, at 1100°C, the origin of the fracture was not found clearly. As the fracture mechanism, intergranular and transgranular fracture

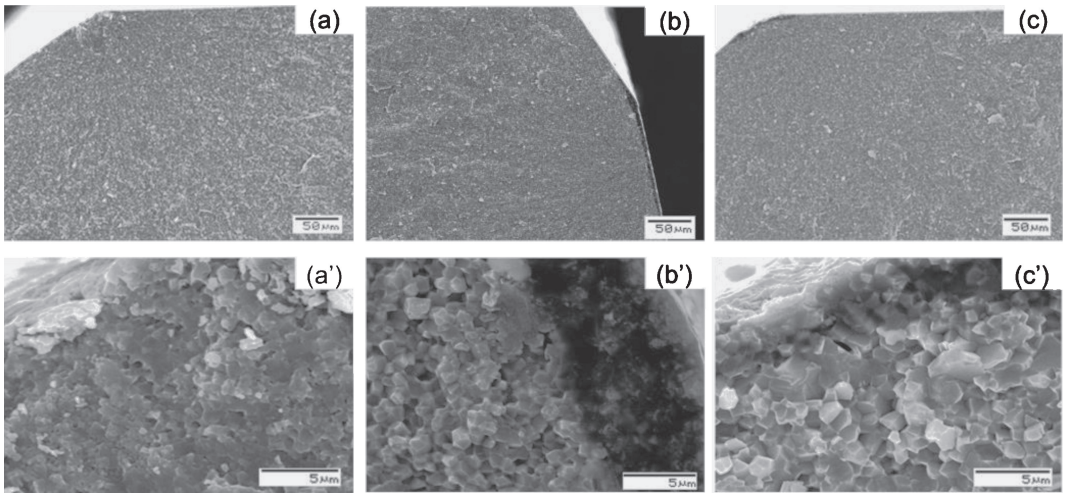

Fig. 5. SEM images of fracture surface of the samples sintered at (a, a′) 1000°C, (b, b′) 1100°C and (c, c′) 1200°C.

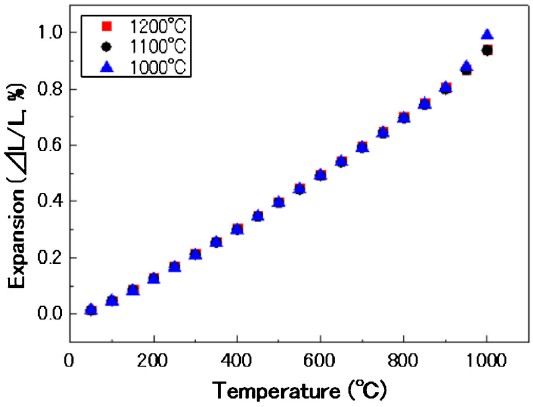

Fig. 6. The expansion ratio of the each sample (ΔL/L, %).

were observed for all samples. The dominant fracture mechanism seems to be changed from transgranular to intergranular fracture with increasing sintering temperature, which can be attributed to the anisotropic thermal stress during the cooling.

Figure 6 shows the bulk thermal expansion at each sample sintered by SPS at 1000–1200°C. The thermal expansion behavior of each sample was almost identical, except at around 1000°C (i.e., close to the sintering temperature). The bulk CTE values of the all SPS samples were $\sim 10 \times 10^{-6}\,K^{-1}$, which confirms the fewness of microcracks compared with ordinary $MgTi_2O_5$ samples with many microcracks. Since the low thermal expansion in polycrystalline $MgTi_2O_5$ is attributed to the microcracks, "high strength" and "low thermal expansion" are in trade-off relationship. Further microstructural control will be needed to break this trade-off.

In this study, $MgTi_2O_5$ ceramics were reactively sintered by SPS from TiO_2 anatase and $MgCO_3$ (basic) powders. XRD analysis revealed that the samples sintered at 1100–1200°C consisted of $MgTi_2O_5$ and trace $MgTiO_3$ phases. High relative density and flexural strength, 99.9% and 341.5 MPa, were obtained for the sample sintered at 1200°C. It was the highest flexural strength among pseudobrookite-type ceramics.

Acknowledgement We thank Prof. Tamotsu Koyano at Cryogenics Division, Research Facility Center, University of Tsukuba for his help on SEM observation. VESTA[19] was used for crystal drawing.

References

1) G. Bayer, *J. Less-Common Met.*, 24, 129–138 (1971).
2) J. F. W. Bowles, *Am. Mineral.*, 73, 1377–1383 (1988).
3) Y. Suzuki and Y. Shinoda, *Sci. Technol. Adv. Mater.*, 12, 034301–034306 (2011).
4) N. E. Brown and A. Navrotsky, *Am. Mineral.*, 74, 902–912 (1989).
5) J. A. Kuszyk and R. C. Bradt, *J. Am. Ceram. Soc.*, 56, 420–423 (1973).
6) R. Maki and Y. Suzuki, *J. Ceram. Soc. Japan*, 121, 568–571 (2013).
7) Y. Ohya, K. Hamano and Z. Nakagawa, *J. Ceram. Soc. Japan*, 94, 665–670 (1986).
8) E. Kato, K. Daimon and J. Takahashi, *J. Am. Ceram. Soc.*, 63, 355–356 (1980).
9) T. S. Liu and D. S. Perera, *J. Mater. Sci.*, 33, 995–1001 (1998).
10) S. M. Lang, C. L. Fillmore and L. H. Maxwell, *J. Res. Natl. Bur. Stand.*, 48, 298–312 (1952).
11) O. Guilllon, J. Gonzalez-Julian, B. Dargatz, T. Kessel, G. Schierning, J. Räthel and M. Herramnn, *Adv. Eng. Mater.*, 16, 830–849 (2014).
12) K. Sairam, J. K. Sonber, T. S. R. Ch. Murthy, C. Subramanian, R. K. Fotedar, P. Nanekar and R. C. Hubli, *Int. J. Refract. Met. Hard Mater.*, 42, 185–192 (2014).
13) B.-N. Kim, E. Prajatelistia, Y.-H. Han, H.-W. Son, Y. Sakka and S. Kim, *Scr. Mater.*, 69, 366–369 (2013).
14) J. Yun, H. Son, E. Prajatelistia, Y. H. Han, S. Kim and B. N. Kim, *Adv. Appl. Ceramics*, 113, 67–72 (2014).
15) Y. Suzuki and M. Morimoto, *J. Ceram. Soc. Japan*, 118, 1212–1216 (2010).
16) Y. Suzuki, T. S. Suzuki, Y. Shinoda and K. Yoshida, *Adv. Eng. Mater.*, 14, 1134–1138 (2012).
17) Y. Nakagoshi and Y. Suzuki, *J. Asian Ceram. Soc.*, 3, 334–338 (2015).
18) Y. Nakagoshi and Y. Suzuki, *Int. Lett. Chem. Phys. Astro.*, 46, 37–41 (2015).
19) K. Momma and F. Izumi, *J. Appl. Cryst.*, 44, 1272–1276 (2011).